Automatic Detection of QRS Complex, P-Wave and T-Wave in the Electrocardiogram

Martin Bachler[1,*], Christopher Mayer[2], Bernhard Hametner[1], Siegfried Wassertheurer[2]

[1] Department of Analysis and Scientific Computing, Vienna University of Technology, Wiedner Hauptstraße 8-10, 1040 Vienna, Austria; *martin.bachler@student.tuwien.ac.at*

[2] AIT Austrian Institute of Technology, Health & Environment Department, Business Unit Biomedical Systems, Muthgasse 11, 1190 Vienna, Austria

Abstract. Every third death in developed countries is caused by cardiac diseases, which are the number one cause of death. Duration and dynamic changes of certain intervals of the ECG are well established indicators in the diagnosis of cardiac diseases. Furthermore, several agencies require the assessment of the effect of newly developed drugs on the QT interval.

Automated measurement and annotation of the ECG shows numerous advantages over manual methods, therefore the long term aim is to develop an all-in-one device for data acquisition and ECG analysis. The development process is conducted in different stages, whereas the first step and short term aim described in this paper consists of creating algorithms in MATLAB® and validating them against ECG signals manually annotated by medical experts. This early stage is followed by porting all algorithms to the aimed platform and finally by hardware-in-the-loop simulations coupling the measurement hardware with the MATLAB® model.

The presented algorithm detects R peaks based on the signals amplitude and first derivative as well as RR intervals. False positive detections due to artifacts are prevented by analyzing the signal's local statistic characteristics. These intermediate results are automatically classified to distinguish normal heartbeats from potential premature ventricular contractions. QRS complexes, P and T waves are detected by their first derivative for each class of heartbeats and are separately refined for each detected heartbeat.

The algorithm has been verified against four PhysioNet databases and achieved a sensitivity of 98.5% and a positive predictive value of 98.3%, respectively.

These results are promising, but further work is still required to implement the algorithm on an embedded system to build an easy to use all-in-one device.

Introduction

Every third death in the United States and actually nearly every second one in Europe is caused by cardiovascular diseases [1, 2]. Their main forms are coronary heart diseases, causing nearly half of all deaths caused by cardiovascular diseases. Coronary heart diseases are the most and second most common cause of death in Europe and the United States, respectively [1, 2].

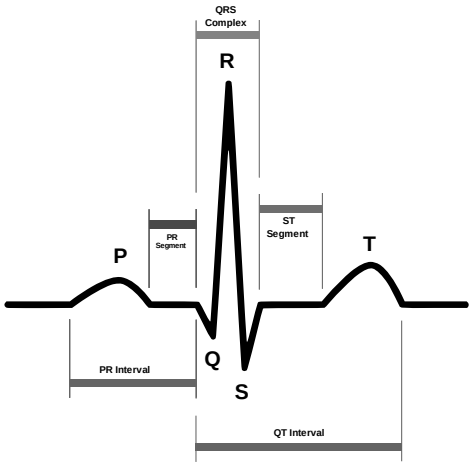

Figure 1. Schematic representation of a normal heartbeat and its features seen on ECG (modified from [3]).

Electrocardiography (ECG) is a widespread, non-invasive and painless technique to measure physiologic activity and pathologic changes of the myocardium. As shown in Figure 1, the tracing of one heartbeat consists of a P wave (atrial depolarization), a QRS complex (ventricular depolarization) and a T wave (ventricular repolarization). Several well-defined segments and intervals between these features are well established indicators in the diagnosis of cardiac diseases, most notably the PR interval (from the onset of the P wave to the onset of the QRS complex) and the QT interval (from the onset of the QRS complex to the offset of the

SNE Simulation Notes Europe – Print ISSN 2305-9974 | Online ISSN 2306-0271
SNE 22(1), 2012, 39-44 | doi: 10.11128/sne.22.tn.10113

T wave). In addition, some non-antiarrhythmic drugs may have the undesired property of prolonging the QT interval, therefore several agencies and national regulators require the assessment of this effect in newly developed drugs [4]. Automated methods for measurement and annotation of the ECG offer several advantages over manuals ones, such as immunity to observer related errors and operator fatigue, higher accuracy in repeated measurements and faster or more extensive testing at lower cost.

In the last decades, a lot of ECG analysis methods have been presented. Especially the rapid development of powerful computing hardware led to a widespread application of software ECG annotation algorithms in the last 30 years. Despite the usage of many different approaches such as signal derivatives [5], digital filters, wavelets [6] and neural networks, most methods focus only on the detection of the QRS complex [7]. Other software algorithms extend existing QRS detectors with the evaluation of QT intervals [8, 9] or P waves [6], but these methods are only suitable for offline ECG analysis. This paper presents an algorithm combining some of these methods and adopting them for online (real time) measurements.

1 Development Process

To facilitate the use of full automatic ECG annotation, the aim is to develop an all-in-one-device for ECG acquisition and analysis. As Figure 2 shows, the process of development is conducted in several stages, starting with offline prototyping and verification using MATLAB®, followed by porting the algorithm to an embedded system and finally performing hardware-in-the-loop simulations to validate the functionality.

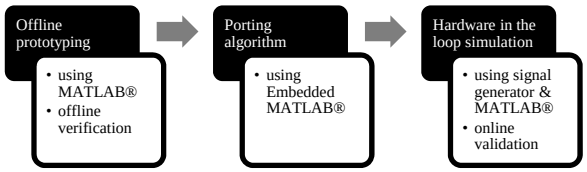

Figure 2. Overview of the development process.

MATLAB®, a numerical computing software developed by MathWorks™, allows easy matrix and vector manipulations and can interface with other programming languages including C. These properties make MATLAB® the ideal choice for rapid development of signal processing algorithms intended to be used on digital signal processors. Besides, based on its scripting features, it allows the automation of the verification process. The developed algorithm has been verified against ECG signals manually annotated by medical experts from different PhysioNet databases [10, 11].

After its successful validation, the algorithm is ported to an embedded system containing a digital signal processor. Embedded MATLAB®, a subset of the MATLAB® language, supports efficient code generation for deployment for embedded systems and therefore is the optimal choice for this task.

Finally the embedded system is validated using a hardware-in-the-loop simulation. In this step, the final system is ready to use, but instead of measuring ECGs in real subjects, they will be simulated using a signal generator controlled by MATLAB®. A hardware-in-the-loop simulation allows the reproduction of previously annotated signals and hence an efficient verification of the results as well as a validation of the final device.

2 Measurement Algorithm

R peaks are the most prominent feature in ECG tracings. Thus they can be used as reference point for further features and are a good choice to start detection with. The measurement algorithm continuously tries to detect them based on the signal amplitude and its first derivative [5]. Local statistics of the signal are evaluated to distinguish correctly detected R peaks from artifacts caused by movements of the subject. Once an R peak is found a classification is applied in real time to separate normal QRS complexes from potential premature ventricular contractions. Creating templates by averaging the signals reduces noise and allows a more accurate detection of all further features. Subsequently, QRS on- and offset are detected based on the signal's local amplitude. T and P waves as well as their on- and offsets are derived based on their first derivatives [9]. QRS on- and offset as well as all parts of T and P waves are primarily detected in the template of their respective class. The actual signal is only used for local refinement.

To detect R peaks, a feature signal is continuously calculated as follows:

- Calculate the first discrete derivative D_t of the signal S_t

$$D_t = S_t - S_{t-1} \tag{1}$$

- Evaluate the amplitudes SA_t of S_t and DA_t of Dt within a moving window (w = 60 ms)

$$SA_t = \max(S_{(t-w)\dots t}) - \min(S_{(t-w)\dots t}) \quad (2)$$

$$DA_t = \max(D_{(t-w)\dots t}) - \min(D_{(t-w)\dots t}) \quad (3)$$

- Combine SA_t and DA_t

$$C_t = SA_t{}^2 \cdot DA_t \quad (4)$$

- Calculate feature signal FSt within a moving window (w = 100 ms)

$$FS_t = \max(C_{(t-w)\dots t}) \quad (5)$$

- Use the mean value of the last 2 seconds of FS_t as threshold Th_t (w = 2 s)

$$Th_t = \frac{1}{w} \sum_{k=t-w}^{t} FS_k \quad (6)$$

Figure 3 shows three different ECG signals (containing noise and small artifacts; high T wave; sudden subject motion) with their corresponding feature signals. The feature signal is robust regarding noise, small artifacts and prominent T waves, but does respond to sudden motion of the subject.

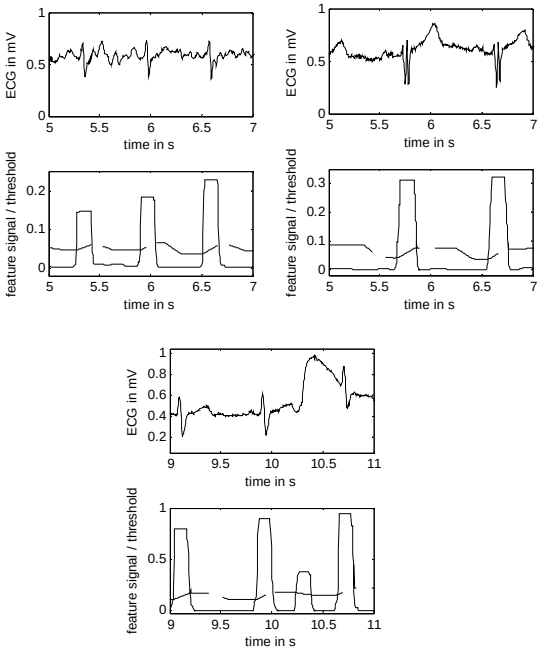

Figure 3. Differently shaped ECG signals with their corresponding response of the feature signal FS_t (equation 5) and its threshold Th_t (equation 6).

Whenever the feature signal exceeds the threshold, the following statistic criterions have to be fulfilled. Otherwise the detected part of the signal is interpreted as an artifact:

- Standard deviation σ within the last 400 ms

$$FS_t > Th_t + 6 \cdot \sigma^3 \quad (7)$$

- Kurtosis β_2 within the last 2.5 seconds

$$\beta_2 > 4 \quad (8)$$

Within each region containing an R peak, differences between local minima and maxima are calculated. The maximum with the highest difference to its surrounding minima is chosen as the exact position of the R peak. If more than two R peaks have already been detected, a template is built by averaging them. The correlation between the newly detected R peak and the template is computed as similarity measure and has to exceed a predefined threshold. Otherwise the R peak is discarded.

To avoid not detecting potentially missed or wrongly discarded R peaks, the intervals between two consecutive R peaks (RR interval) are calculated. If one RR interval exceeds 1.8 times the previous ones, the section between those R peaks is searched again with lower thresholds.

Classification of the R peaks is performed in real time. The ECG signal at each R peak ± 0.5 seconds is compared to a predefined number of classes using correlation and is assigned to its most similar class. If classes among each other correlate better than with the current R peak, these classes are merged and a new class is created from the current signal. This approach results in dynamically evolving classes, continuously enhancing with the duration of the measurement.

To reduce noise, templates are created by averaging each class and are used for the detection of all subsequent features (QRS on- and offset, P and T wave as well as their on- and offsets). Only a local refinement is performed using the original signal.

To detect the onset of the QRS complex, an interval of 150 ms straight before the R peak of the template is analyzed as follows:

- Calculate the amplitudes TAt and TDAt of the template Tt and its first discrete derivate within a moving window (w = 30 ms)

$$TA_t = \max(T_{(t-w)\dots t}) - \min(T_{(t-w)\dots t}) \quad (9)$$

$$TDA_t = \max(T'_{(t-w)\dots t}) - \min(T'_{(t-w)\dots t}) \quad (10)$$

- Calculate a threshold TT and TD for the amplitudes TA_t and TDA_t

$$\mathrm{TT} = \mathrm{c}_1 \cdot (\max(TA_\mathrm{t}) - \min(TA_\mathrm{t})) + \min(TA_\mathrm{t}) \quad (11)$$

$$\mathrm{TD} = \mathrm{c}_2 \cdot (\max(TDA_\mathrm{t}) - \min(TDA_\mathrm{t})) + \min(TDA_\mathrm{t}) \quad (12)$$

with c_1 and c_2 being predefined constants.

- The point closest to the R peak, where TA_t is below TT or TDA_t is below TD is marked as reference for the QRS onset.
- The exact QRS onset is found within a 40 ms region prior to the reference point at the closest extremum to the R peak in the original signal. If no extremum is present, the point with the lowest slope is considered to be the QRS onset.

The computation of the QRS offset is very similar to the onset, with two exceptions:

- In order to annotate prolonged QRS complexes correctly, the analyzed interval is chosen larger.
- In equation (9) and (10), window w is 60 ms.

The peak of the T wave is detected by a special 'wings' function W as described by Christov and Simova [9] as follows:

$$\mathrm{W}_1 = \mathrm{T}_{\mathrm{t}-40\mathrm{ms}} - \mathrm{T}_\mathrm{t} \quad (13)$$

$$\mathrm{W}_2 = \mathrm{T}_\mathrm{t} - \mathrm{T}_{\mathrm{t}+40\mathrm{ms}} \quad (14)$$

$$\mathrm{W} = \mathrm{W}_1 \cdot \mathrm{W}_2 \quad (15)$$

The 'wings' function is applied to the template Tt between the previously detected QRS offset and the end of the template (0.5 seconds after the R peak). As shown in Figure 4, the position of the minimum of the 'wings' function represents the peak of the T wave, regardless of the polarization of the T wave. Subsequently, the position of the peak of the T wave is refined using the original signal by finding a local minimum or maximum, depending on the wave's polarization.

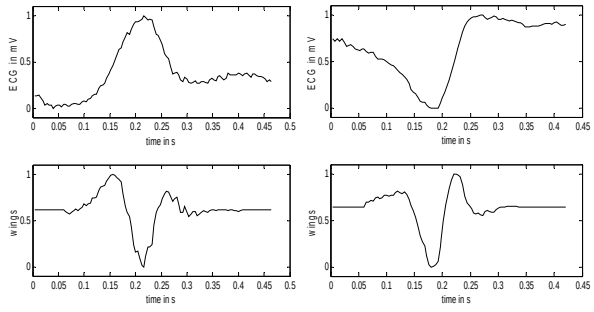

Figure 4. Top: Different T waves (left: positive T wave, right: negative T wave). Bottom: corresponding 'wings' function.

The part of the template between QRS offset and T peak is searched for the closest extremum to the T peak, which is used as reference point for T onset. If no extremum is present, the point with the flattest slope is used instead. Like the T peak, the T onset is refined by finding a local extremum in the original signal. In some cases, especially in ECG traces showing prolonged duration of the QRS complex, T wave and QRS complex overlap. In this case, no reasonable T onset point can be found, even not by medical experts. This condition leads to detection of the T onset straight before the T peak, allowing easy recognition. In this case, no T onset will be annotated at all.

The detection of the T offset is performed in a similar manner between the T peak and the end of the template (0.5 seconds after the R peak).

To detect the peak of the P wave, the interval between the preceding T offset and the current QRS onset is evaluated in the template by a slightly altered 'wings' function (equation 13, 14, 15) which responds just to positive peaks. Again, the peak is located at the minimum of the 'wings' function. P onset and P offset are found in the same way as T onset and T offset.

Due to very small amplitude or high noise level, the P wave in some ECG recordings is indiscernible. To prevent the algorithm from false detections, the amplitude of the P wave (derived as difference in voltage between the P peak and the mean of P onset and P offset) has to exceed a certain fraction of the amplitude of the QRS complex, otherwise no P wave (peak, onset and offset) is detected at all.

3 Results

PhysioNet databases are a collection of recordings of different physiological modalities such as electroencephalogram, electrocardiogram, blood pressure, respiration and others. Depending on their objective, several databases contain different kinds of annotations [10, 11]. Hence, annotations done by medical experts can be used to verify automated algorithms. The following databases have been chosen for the verification of the algorithm presented in this paper due to a wide range of different ECG signals as well as a reasonable amount of expert annotations:

- QT Database, created to evaluate algorithms detecting the QT interval [12].
- AF Termination Challenge Database, designed to be used in 'Computers in Cardiology Challenge 2004'.

- MIT-BIH Arrhythmia Database, test material for evaluation of arrhythmia detectors.
- Fantasia Database, originally used for testing automated arrhythmia detection [13].

The presented algorithm was tested against all four databases with respect to the detection rate of QRS complexes. The American National Standards Institute (ANSI) essentially recommends two parameters for the evaluation of the detection rate [14]: the sensitivity *Se*

$$Se = \frac{TP}{TP + FN} \tag{16}$$

and the positive predictive value *PPV*

$$PPV = \frac{TP}{TP + FP} \tag{17}$$

where *TP* is the number of true positive, *FN* the number of false negative and *FP* the number of false positive detections.

A sensitivity of 98.5% and a positive predictive value of 98.3% were achieved in the verification of the detection rate. Time differences between detected and corresponding annotated points of the QT database are shown in Table 1. Durations of the PR interval, the QRS complex and the QT interval were calculated from the results of the algorithm and the expert annotations, respectively. The differences between the results of the algorithm and the annotations are shown in Figure 5 as Bland-Altman diagrams [15]. Mean and standard deviation of these differences are -1.1 ± 19.9 ms for the PR interval, 3.6 ± 16.5 ms for the QRS complex and -4.8 ± 35.3 ms for the QT interval. These results are satisfying and match existing offline algorithms [7, 8, 16].

	Algorithm-expert deviation		**Inter-expert deviation**	
Feature	**Mean**	**Std**	**Mean**	**Std**
P onset	2.3 ms	23.8 ms	*	*
P peak	0.5 ms	22.2 ms	*	*
P offset	- 0.3 ms	27.2 ms	*	*
QRS onset	0.5 ms	10.2 ms	3.8 ms	14.2 ms
R peak	- 9.1 ms	14.4 ms	0.1 ms	2.4 ms
QRS offset	4.3 ms	12.5 ms	2.7 ms	17.0 ms
T onset	10.8 ms	63.0 ms	9.5 ms	44.9 ms
T peak	- 3.3 ms	33.1 ms	3.5 ms	30.0 ms
T offset	- 4.2 ms	38.8 ms	5.8 ms	39.9 ms

Table 1: Means and standard deviations of differences in time between annotated and detected points as well as between different expert annotations. (* Annotated by one expert only).

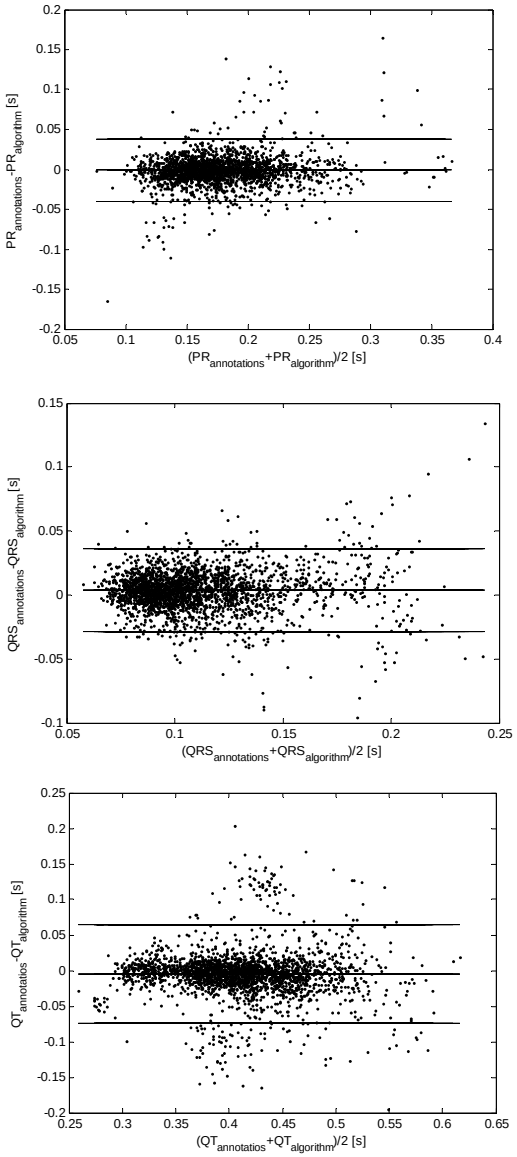

Figure 5. Bland-Altman diagrams comparing the duration of certain intervals derived from expert annotations with the results of the algorithm. Top left: PR interval. Top right: QRS complex. Bottom: QT interval.

4 Discussion and Conclusion

In most cases, the average deviations shown in Table 1 are in the range of the sampling interval of 4 ms, suggesting an insignificant error. The standard deviations of the differences between algorithm results and expert annotations also match with those of inter-expert annotations. Reflecting the uncertainty regarding the exact position of these features among experts, these results suggest that the presented algorithm performs approximately as well as humans.

The two outliers in Table 1, R peak and T onset, are partially arising from bad or unusual annotations in the QT Database. R peaks are sometimes annotated at negative peaks within the QRS complex, whereas they ought to be positive by definition. The position of the T onset point is often ambiguous due to overlapping of the T wave with the QRS complex. This fact is also reflected by the high standard deviation of the inter-expert deviations. Nevertheless, even unambiguous T onset points often have not been annotated in the QT database, making reasonable comparison with the algorithm difficult.

Bland-Altman diagrams comparing the annotated and calculated durations of the PR interval, the QRS complex and the QT interval in Figure 5 do not show any trends and thus do not suggest any methodical error. Their means and standard deviations are in the same range as those in Table 1 and therefore do not show any abnormalities.

The results of the offline verification process are promising. Further work is required to implement the algorithm on an embedded system and run hardware-in-the-loop simulations for validation in order to build an all-in-one device for ECG measurement with real time annotation.

References

[1] V.L. Roger, A.S. Go, D.M. Lloyd-Jones, R.J. Adams, J.D. Berry, T.M. Brown, M.R. Carnethon, S. Dai, G. de Simone, E.S. Ford, and others*: Heart disease and stroke statistics-2011 update: A report from the American Heart Association.* Circulation 123 (2011), e18-e209.

[2] S. Allender, P. Scarborough, V. Peto, M. Rayner, J. Leal, R. Luengo-Fernandez, and A. Gray: *European cardiovascular disease statistics*. European Heart Network (2008)

[3] A. Atkielski: *SinusRhythmLabels.* http://en.wikipedia.org/wiki/File:SinusRhythmLabels.svg (23:40, 13 January 2007).

[4] U.S. Department of Health and Human Services - Food and Drug Administration and Center for Drug Evaluation and Research (CDER) and Center for Biologics Evaluation and Research (CBER): *Guidance for Industry: E14 Clinical Evaluation of QT/QTc Interval Prolongation and Proarrhythmic Potential for Non-Antiarrhythmic Drugs*. Regulatory Information (10 2005).

[5] V.S. Chouhan, and S.S. Mehta: *Detection of QRS complexes in 12-lead ECG using adaptive quantized threshold*. IJCSNS 8 (2008), 155-63.

[6] A. Diery, D. Rowlands, T.R.H. Cutmore, and D. James: *Automated ECG diagnostic P-wave analysis using wavelets*. Computer Methods and Programs in Biomedicine (2010).

[7] B.U. Köhler, C. Hennig, and R. Orglmeister: *The principles of software QRS detection*. IEEE Engineering in Medicine and Biology Magazine 21 (2002), 42-57.

[8] D. Hayn, A. Kollmann, and G. Schreier: *Automated QT interval measurement from multilead ECG signals*. Computers in Cardiology (2008), 381-384

[9] I. Christov, and I. Simova: *Fully automated method for QT interval measurement in ECG*. Computers in Cardiology (2008), 321-324

[10] A.L. Goldberger, L.A.N. Amaral, L. Glass, J.M. Hausdorff, P.Ch. Ivanov, R.G. Mark, J.E. Mietus, G.B. Moody, C.-K. Peng, and H.E. Stanley: *PhysioBank, PhysioToolkit, and PhysioNet: Components of a New Research Resource for Complex Physiologic Signals*. Circulation 101 (2000), e215-e220

[11] PhysioNet: *PhysioBank.* http://physionet.org/ physiobank/database (19:21, 15 April 2011).

[12] P. Laguna, R.G. Mark, A. Goldberg, and G.B. Moody: *A database for evaluation of algorithms for measurement of QT and other waveform intervals in the ECG*. Computers in Cardiology (1997), 673-676.

[13] N. Iyengar, C.-K. Peng, R. Morin, A.L. Goldberger, and L.A. Lipsitz: *Age-related alterations in the fractal scaling of cardiac interbeat interval dynamics.* American Journal of Physiology 271 (1996), R1078-R1084

[14] ANSI/AAMI EC57: *Testing and reporting performance results of cardiac rhythm and ST segment measurement algorithms*. AAMI Recommended Practice/American National Standard (1998). Available: http://www.aami.org; Order Code: EC57-293.

[15] J.M. Bland and D.G. Altman: *Statistical methods for assessing agreement between two methods of clinical measurement*. The LANCET 1 (1986), 307-310

[16] G. Schreier, D. Hayn, and S. Lobodzinski: *Development of a new QT algorithm with heterogenous ECG databases*. Journal of electrocardiology 36 (2003), 145-150.

Submitted: October 2011
Revised: January 2012
Accepted: March 15, 2012